https://doi.org/10.5194/ar-2026-45
Preprint. Discussion started: 17 November 2026
© Author(s) 2026. CC BY 4.0 License.



AEROSOL Research Discussions

Understanding distribution patterns of secondary inorganic aerosols in two distinct environments through statistical learning

Zehao Zou[1,2], Wei Du[3], Giancarlo Ciarelli[2,4], Yongchun Liu[1], Chao Yan[4], Jing Cai[5], Qiaozhi Zha[4], Kaspar Rudolf Daellenbach[6], Men Xia[1,2,4], Xinran Zhang[2], Qi Yuan[1,2], Tinghan Zhang[2], Feixue Zheng[1], Yuzheng Wang[1], Chenjie Hua[1], Zongcheng Wang[1], Hongyu Pang[1], Boying Song[1], Li Ma[1], Wenshuo Zhou[1], Junlei Zhan[1], Wei Ma[1], Tuukka Petäjä[2], Nina Sarnela[2], Ilona Jaakkola[2], Lauri Ahonen[2], Veli-Matti Kerminen[2], Markku Kulmala[1,2,4], and Tom Kokkonen[2,4]

[1]Aerosol and Haze Laboratory, Beijing Advanced Innovation Center for Soft Matter Science and Engineering, Beijing University of Chemical Technology, Beijing, 100029, China
[2]Institute for Atmospheric and Earth System Research, University of Helsinki, Helsinki, 00014, Finland
[3]State Key Laboratory of Atmospheric Environment and Extreme Meteorology, Institute of Atmospheric Physics, Chinese Academy of Sciences, Beijing, 100029, China
[4]Nanjing-Helsinki Institute in Atmospheric and Earth System Sciences, Nanjing University, Nanjing, 210023, China
[5]School of Atmospheric Physics, Nanjing University of Information Science and Technology, Nanjing, 210044, China
[6]Paul Scherrer Institute PSI, Forschungsstrasse 111, 5232 Villigen PSI, Switzerland

Correspondence: Wei Du (wei.du@helsinki.fi)

Abstract. Sulfate and nitrate are major components of fine particulate matter, yet their concentration patterns and associated environmental factors remain insufficiently understood across contrasting environments. We analyzed observations from urban Beijing, China (2018–2022), and the boreal forest in Hyytiälä, Finland (2018–2021). Gaussian mixture modeling and partial least squares discriminant analysis were combined to identify concentration regimes and assess the relative importance of environmental variables. Both compounds exhibited unimodal, lognormal-like concentration distributions in Hyytiälä and multimodal distributions in Beijing. In Beijing, concentrations of both compounds declined over the study period. From low to high concentration regimes, the relative importance of predictors shifted from gaseous precursors to air mass transport and relative humidity. This study provides a transferable statistical framework for characterizing aerosol pollution regimes and their associated environmental conditions.

1 Introduction

Fine particulate matter affects air quality, visibility, climate, and human health (Cao et al., 2012; Feng et al., 2021). Sulfate (SO_4) and nitrate (NO_3) are two major secondary inorganic aerosol components therein (Ervens, 2015; Xie et al., 2023). These two compounds are formed through different but coupled atmospheric pathways. SO_4 is produced from SO_2 oxidation through gas phase, aqueous phase, and heterogeneous reactions, while NO_3 is mainly produced from HNO_3 formation through the oxidation of NO_2 by OH under sunlit conditions and from N_2O_5 hydrolysis under dark conditions, followed by gas-particle partitioning (Liu et al., 2021a; Zhang et al., 2015). These processes are regulated by precursor availability, atmospheric

https://doi.org/10.5194/ar-2026-45
Preprint. Discussion started: 17 November 2026
© Author(s) 2026. CC BY 4.0 License.



AEROSOL Research Discussions

oxidizing capacity, temperature, humidity, and air mass history (Cao et al., 2020; Vasilakos et al., 2018; Guo et al., 2017; Xie et al., 2026).

The processes and factors controlling SO_4 and NO_3 formation are expected to differ between anthropogenic and biogenically dominated environments because their precursor source structures, aerosol loading, humidity regimes, and transport histories differ strongly (Liu et al., 2020a; Kulmala et al., 2025). Meanwhile, understanding how these factors will change with anthropogenic emissions is crucial. China has experienced major changes in aerosol composition following stringent emission controls, especially after the implementation of the Air Pollution Prevention and Control Action Plan in 2013 (Zheng et al., 2018; Geng et al., 2019). Previous studies reported substantial decreases in particulate SO_4, while NO_3 became increasingly important in $PM_{2.5}$ (Sun et al., 2020). This shift could be attributed to the combined effects of uneven reductions in precursor emissions, changes in atmospheric oxidizing capacity, and the resulting complex responses of secondary aerosol formation (Sun et al., 2020; Meng et al., 2022; Li et al., 2022; Wang et al., 2020). However, the drivers of the long-term evolution of SO_4 and NO_3 have not yet been fully quantified.

Here, we compared SO_4 and NO_3 observations in Beijing and Hyytiälä during 2018–2022 and 2018–2021, respectively, representing anthropogenically influenced and boreal forest background environments (Kulmala et al., 2025; Heikkinen et al., 2020). We introduced a statistical framework that combines Gaussian mixture models (GMMs) to identify concentration regimes with partial least squares discriminant analysis (PLS-DA) for environmental driver analysis. By combining chemical, meteorological, and trajectory-based indicators, we determined how the rates and pathways of SO_4 and NO_3 formation differ between the two environments, how they have evolved in recent years and how their controlling factors are regime dependent.

2 Materials and Methods

2.1 Data and Instruments

We compared high-resolution ambient observations from two contrasting environments: the Aerosol and Haze Laboratory at the west campus of Beijing University of Chemical Technology in Beijing, China (AHL/BUCT; 39.942° N, 116.298° E; Liu et al., 2020b), and the SMEAR II station in the Finnish boreal forest in Hyytiälä, Finland (61.846° N, 24.295° E; Hari et al., 2013). Meteorological variables, gaseous precursors, and particulate SO_4 and NO_3 were measured at both sites. Instrument intercomparisons and/or calibrations were conducted during the observation periods to ensure instrument stability (Kulmala et al., 2025; Righi et al., 2026). Details of the measurement setup and data availability are provided in Text S1. Sulfur oxidation ratio (SOR) and nitrogen oxidation ratio (NOR) were calculated on a molar concentration basis after unit harmonization to describe the partitioning of sulfur and nitrogen between gaseous precursors and particulate products. The combined molar concentrations of gaseous precursors and particulate products, S_{tot} = [SO_2] + [SO_4] and N_{tot} = [NO_2] + [NO_3], are defined in Text S2.

https://doi.org/10.5194/ar-2026-45
Preprint. Discussion started: 17 November 2026
© Author(s) 2026. CC BY 4.0 License.



AEROSOL Research Discussions

2.2 Trajectory-Based Air Mass Exposure

Air mass transport histories from 2018 to 2022 were analyzed at both stations using 96 h backward trajectories calculated with the HYSPLIT model (Stein et al., 2015) and archived meteorological data from the Global Data Assimilation System (GDAS; $1^\circ \times 1^\circ$; National Centers for Environmental Prediction, n.d.). To quantify the influence of air mass transport, two trajectory-based indicators were used to characterize air mass exposure: Time over Populated Land (ToPL) for Beijing and Time over Land (ToL) for Hyytiälä. ToPL was used to represent exposure to densely populated East Asian source regions (Hakala et al., 2022), whereas ToL was used to describe land-influenced transport before arrival at Hyytiälä following the sector framework described previously (Tunved et al., 2006; Petäjä et al., 2022). For Hyytiälä, only observations classified into the clean trajectory sector were included and used as a boreal background reference subset. Details of the trajectory calculation, source-region definitions, and clean sector filtering are provided in Text S3.

2.3 Statistical Learning

To identify concentration regimes, Gaussian mixture models (GMMs) were fitted to $\log_{10}$-transformed $[SO_4]$ and $[NO_3]$ independently for each year and compound. We compared Bayesian information criterion (BIC) values and fitted concentration distributions and selected four regimes to describe the main distributional features using the same number of groups in each year. Partial least squares discriminant analysis (PLS-DA) was then used to identify variables associated with differences between adjacent concentration regimes. Variable importance in projection (VIP) scores were used to evaluate the relative contribution of each predictor to the PLS-DA classification and identify the variables most important for distinguishing concentration regimes (Haque et al., 2025). Variables with VIP greater than 1 were considered important contributors to regime separation, following a commonly used empirical criterion (Mahieu et al., 2023). Details of the GMM and PLS-DA procedures are provided in Text S4. GMMs were previously applied in air quality studies (Gómez-Losada et al., 2014; Wang et al., 2024), while PLS-DA has been used in biomedical and chemometric studies (Haque et al., 2025; Mahieu et al., 2023; Land et al., 2011). In this study, combining these methods helped characterize concentration regimes and their associated environmental factors, providing insights into the evolution of sulfate and nitrate concentrations over multiple years.

3 Results and Discussion

3.1 Concentration Distributions

In general, Beijing exhibited substantially higher $[SO_4]$ and $[NO_3]$ than Hyytiälä throughout the study period (Figure 1). The medians were 2.0 $\mu g\,m^{-3}$ for $[SO_4]$ and 3.9 $\mu g\,m^{-3}$ for $[NO_3]$, which were 4.8 and 32.5 times those in Hyytiälä, respectively, reflecting a large contrast between anthropogenic-emission and biogenic-emission dominated environments.

During 2018–2021, $[SO_4]$ in Hyytiälä remained comparatively low and stable and exhibited a relatively narrow, lognormal-like concentration distribution, with annual median values generally below 0.6 $\mu g\,m^{-3}$. Together with the high SOR (median: 0.9), these features suggest that SO_4 in Hyytiälä was highly aged and could mainly be attributed to long-range transport,

https://doi.org/10.5194/ar-2026-45
Preprint. Discussion started: 17 November 2026
© Author(s) 2026. CC BY 4.0 License.

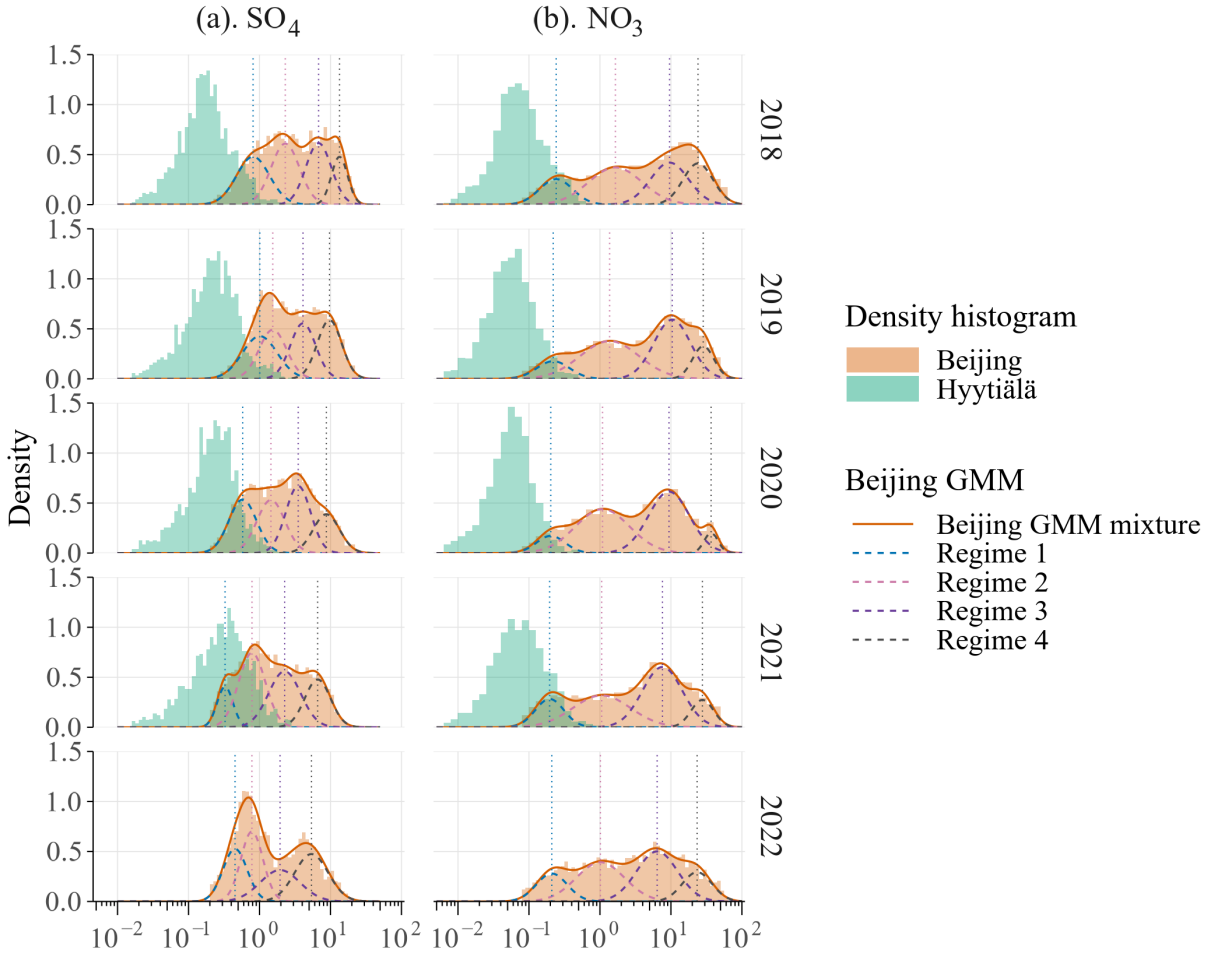


Figure 1. Annual distributions of particulate (a) sulfate and (b) nitrate concentrations in Beijing (2018–2022) and the Hyytiälä clean-sector subset (2018–2021). Concentrations are expressed in $\mu g\,m^{-3}$. Histograms show probability densities of $\log_{10}$-transformed concentrations. For Beijing, solid lines show the fitted GMM densities, dashed lines show mixing-weighted component contributions, and dotted vertical lines mark component medians (10^{μ_k}). Each histogram and total mixture density integrates to 1 on the $\log_{10}$ concentration scale; component areas equal their mixing proportions. The horizontal axis shows the original concentration scale with logarithmic ticks.

consistent with previous studies (Heikkinen et al., 2020; Neefjes et al., 2022). In contrast, $[SO_4]$ in Beijing showed a multi-
80 modal distribution and a significant declining trend in monthly median concentrations over the study period (linear regression: $p < 0.001$; Figure S6). From 2018 to 2022, the annual median $[SO_4]$ decreased by approximately 61%, from 3.0 to 1.2 $\mu g\,m^{-3}$. The observed sulfate decline is consistent with previous reports of sustained reductions following emission-control measures in Beijing (Xu et al., 2019; Yu et al., 2022; Han et al., 2020). Over the past five years, S_{tot} decreased alongside $[SO_4]$, while $[SO_2]$ remained comparatively stable (Figure S7 and Table S1). As a result, SOR decreased from 0.65 in 2018 to 0.51 in 2022

https://doi.org/10.5194/ar-2026-45
Preprint. Discussion started: 17 November 2026
© Author(s) 2026. CC BY 4.0 License.



AEROSOL Research Discussions

(Table S1), likely suggesting that the continued reduction of SO_4 during these years might also be associated with the lower oxidation of sulfur.

With a unimodal distribution, $[NO_3]$ in Hyytiälä (median value $< 0.2\ \mu g\,m^{-3}$) was lower than $[SO_4]$ during 2018–2021. The median NOR ranged from 0.14 to 0.18, indicating a relatively low and stable NO_3 oxidation fraction in Hyytiälä, consistent with weak local NO_3 production under background conditions (Kulmala et al., 2025). In Beijing, monthly median $[NO_3]$ also declined significantly during 2018–2022 (linear regression, $p = 0.007$; Figure S6), while the annual median decreased by 39%, from 4.8 to 2.9 $\mu g\,m^{-3}$. Over the same period, median $[NO_x]$ declined from 19.2 to 10.0 ppb (Table S1), accompanied by a decrease in N_{tot} (Figure S7), whereas NOR showed only modest interannual variation. The lower and upper quartiles of NOR in Beijing over the study period were 0.07 and 0.37, respectively, indicating a broad distribution of oxidation ratios. Together, these results likely suggest that the decrease of $[NO_3]$ in Beijing was mainly in response to reduced NO_x availability instead of changes in NOR. The decline in $[NO_3]$ was smaller than that in $[SO_4]$, and nitrate therefore became increasingly important in $PM_{2.5}$ composition under continued emission controls in China (Wang et al., 2022b; Liu et al., 2021b).

3.2 Regime Separation and Driving Factors

Although both SO_4 and NO_3 decreased significantly over the past five years in Beijing, their annual distributions consisted of multiple recurring regimes, unlike the continuous, unimodal spectra observed for the selected clean air masses arriving at Hyytiälä. The evolution of the distribution modes indicates an ongoing reorganization of aerosol composition as total particle mass decreases in Beijing (Wang et al., 2020, 2022a). To further improve air quality, it is important to distinguish these concentration regimes and identify their associated environmental variables, using GMM followed by PLS-DA. We compared models with one to ten components (Figure S2) and used the selected four regimes in the following analyses.

These regimes were numbered 1 to 4 in ascending order of median concentration. Further, VIP scores were calculated to identify variables distinguishing each concentration regime from the adjacent higher regime (Text S4). For SO_4, the GMM-derived median concentrations of regimes 1–4 were 0.8, 2.3, 6.8, and 13.4 $\mu g\,m^{-3}$ in 2018, compared with 0.5, 0.8, 1.9, and 5.4 $\mu g\,m^{-3}$ in 2022 (Table S2). The regime-specific environmental conditions generally followed a clear pattern: regime 1 was associated with low RH, ToPL, and $[SO_2]$, together with high wind speed, while regime 4 was associated with high RH and ToPL and lower wind speed (Table S3). We noted that RH (76%) in regime 4 in 2020 was the highest among the five years, whereas ToPL did not differ notably from that in the other years, suggesting a possible role of liquid-phase reactions, since particles could be in the liquid phase when RH is higher than 60% in Beijing (Liu et al., 2017).

As shown in Figure 2, for the 1–2 regime transition, SO_2 generally showed the highest VIP scores, followed by ToPL. RH exceeded the VIP = 1 threshold only in 2018 and 2020, while VIP scores for the other variables were generally below 1 during the 1–2 regime transition. Under heavier pollution conditions, represented by the 3–4 transition, ToPL and RH were generally more important than in the 1–2 transition, whereas SO_2 contributed little or no separation at this stage. Among the study years, 2020 was particularly distinct: RH showed high importance across all transitions, including 1–2, whereas the mean VIP score of SO_2 across these three comparisons was approximately 0.5. These results indicate that the occurrence of heavy pollution is usually related to the cumulative effects of air masses exposed to polluted source regions and high-humidity conditions (3–4

https://doi.org/10.5194/ar-2026-45
Preprint. Discussion started: 17 November 2026
© Author(s) 2026. CC BY 4.0 License.

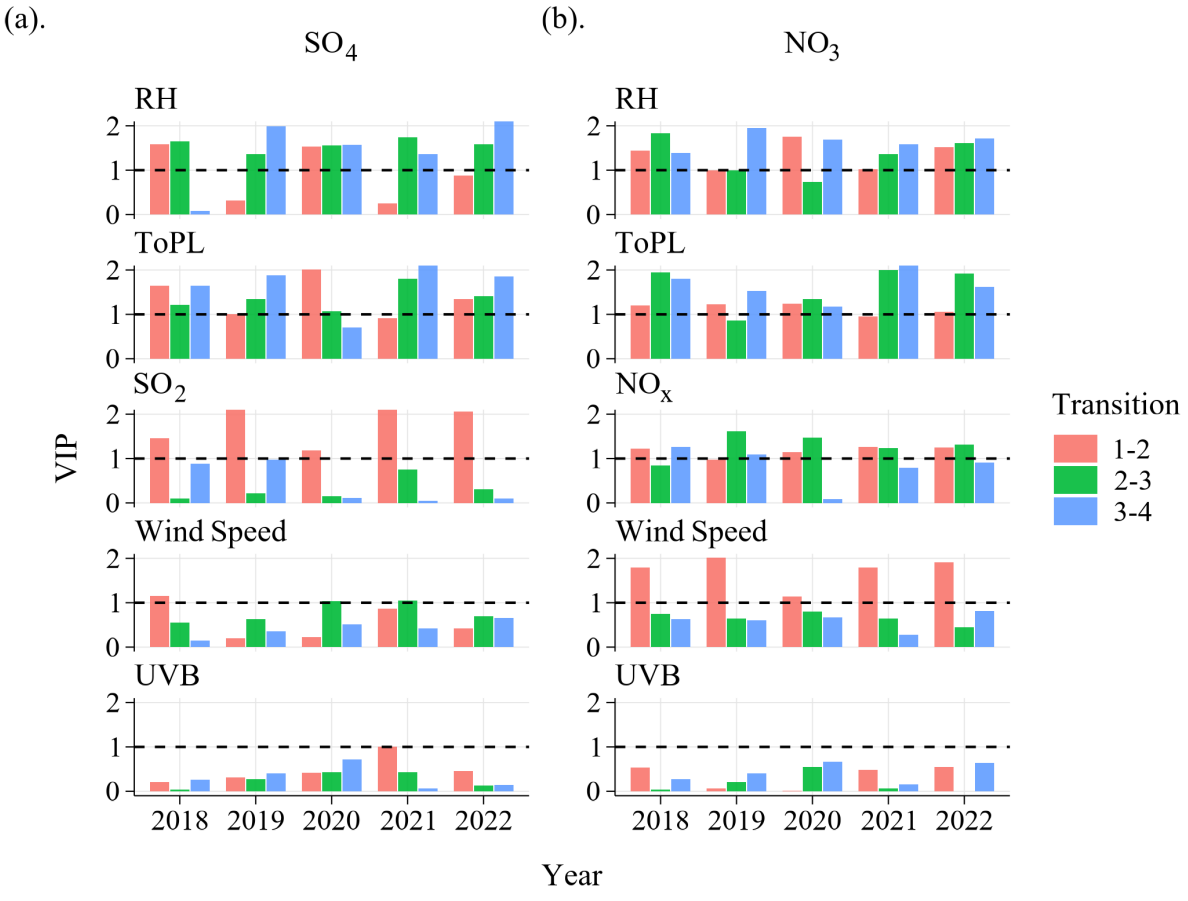


Figure 2. VIP scores derived from PLS-DA for key meteorological and chemical predictors associated with sulfate (SO_4) and nitrate (NO_3) concentration regimes in Beijing (2018–2022). The x-axis represents year, and the y-axis shows VIP scores. Colors denote pairwise comparisons between adjacent GMM derived regimes (1–2, 2–3, and 3–4 regime transitions). The dashed line indicates the VIP = 1 threshold for variable relevance.

transition). A previous study in Beijing emphasized that SO_4 formation is strongly modulated by aerosol phase conditions, including aerosol liquid water and acidity, which makes humid episodes more favorable for multiphase SO_4 production rather than being determined by SO_2 abundance alone (Wang et al., 2023).

For NO_3, the regime structure remained relatively more stable than that of SO_4 from 2018 to 2022, with a gradual weakening of regimes 2 and 3. The corresponding GMM-derived median concentrations were 0.2, 1.7, 9.6, and 24.1 $\mu g\,m^{-3}$ in 2018, and 0.2, 1.0, 6.4, and 23.4 $\mu g\,m^{-3}$ in 2022 (Table S2). As with SO_4, progression from regime 1 to regime 4 in NO_3 was generally accompanied by increasing NO_x, ToPL, and RH, together with decreasing wind speed (Table S3). A notable exception occurred

https://doi.org/10.5194/ar-2026-45
Preprint. Discussion started: 17 November 2026
© Author(s) 2026. CC BY 4.0 License.



AEROSOL Research Discussions

in 2020, when the median NO_x in regime 4 (25.6 ppb) was nearly identical to that in regime 3 (23.0 ppb), whereas the other years showed a clearer monotonic gradient; the remaining variables did not exhibit equally distinct anomalies.

For the NO_3 1–2 transition, wind speed showed the strongest influence (mean VIP = 1.73), followed by RH and ToPL, with mean VIPs of 1.35 and 1.14, respectively. NO_x also showed VIP scores higher than 1 in 2018 and 2020 to 2022. For the 3–4 regime transition, RH had the highest mean VIP score (1.67), followed by ToPL (1.66). Wind speed and NO_x became less relevant, with mean VIP scores below 1. The year 2020 also stood out: during the 1–2 transition, wind speed had its lowest VIP score and RH its highest across the study years. The role of wind speed emphasized that, compared to SO_4, NO_3 was also affected by precursors from local sources such as traffic. Overall, the effects of environmental variables on Beijing's pollution structure did not contribute equally across pollution levels. At low concentrations, the structure was more strongly influenced by gas-phase precursors or wind speed (particularly for NO_3), whereas under high pollution conditions, it was dominated mainly by regional transport and reaction conditions such as RH, providing favorable conditions for heterogeneous reactions.

3.3 The Influence of RH During Air Mass Transport

We further examined how SO_4 and NO_3 varied across RH classes during air mass transport (Figure 3). In general, both $[SO_4]$ and $[NO_3]$ increased with ToPL in Beijing and ToL in Hyytiälä across RH classes, but the underlying controlling mechanisms differed.

In Beijing, $[SO_4]$ was higher under more humid conditions, and the fitted slope of bin-median $[SO_4]$ against ToPL increased from 0.04 $\mu g\,m^{-3}\ h^{-1}$ under low RH to 0.06 $\mu g\,m^{-3}\ h^{-1}$ under high RH. The results indicate that, even when the air mass stays in the populated region for the same duration, the accumulation of $[SO_4]$ will increase significantly with the rise in humidity. This is because the higher RH promoted heterogeneous reactions, allowing SO_2 to be oxidized more efficiently, and hence showed higher SOR (Figure S4), which almost stabilized at 0.7 when $RH > 60\%$. In Hyytiälä, $[SO_4]$ also showed an increasing trend with ToL, while it had limited variations across all RH classes. The SOR remained generally high (> 0.7, Figure S4), indicating that the air masses containing SO_4 were already highly aged before arriving at Hyytiälä. Therefore, the increase of $[SO_4]$ in Hyytiälä was mainly attributable to the air mass accumulation. Due to the different behaviors under different RH during air mass transport, the ratios of $[SO_4]$ between Beijing and Hyytiälä were higher under higher RH.

In Beijing, $[NO_3]$ and NOR increased with ToPL, while $[NO_x]$ remained relatively stable at approximately 20 ppb across all RH conditions (Figure 3 and S5). Given that NO_x typically has an atmospheric lifetime of several hours, longer ToPL could promote particulate NO_3 accumulation rather than the accumulation of NO_x itself (Laughner and Cohen, 2019). The increase in $[NO_3]$ was faster under higher RH, with the fitted slope increasing from 0.07 at low RH ($RH < 40\%$) to 0.18 $\mu g\,m^{-3}\ h^{-1}$ at high RH ($RH > 60\%$), suggesting a more important role of N_2O_5 hydrolysis under higher RH conditions (Liu et al., 2020a). In contrast to Beijing, the separation of $[NO_3]$ among RH classes was not apparent in Hyytiälä, and NOR showed the opposite RH dependence (Figure S5). Under more humid conditions, higher $[NO_x]$ but lower NOR indicated that nitrogen remained predominantly in the gas phase. This could be because the N_2O_5 hydrolysis played a limited role due to the limited particle loading in Hyytiälä, and photochemical NO_3 production under high RH was suppressed due to the low solar radiation. The Beijing-Hyytiälä ratio of $[NO_3]$ generally decreased with increasing ToPL/ToL when $RH < 60\%$, while it was relatively stable

https://doi.org/10.5194/ar-2026-45
Preprint. Discussion started: 17 November 2026
© Author(s) 2026. CC BY 4.0 License.

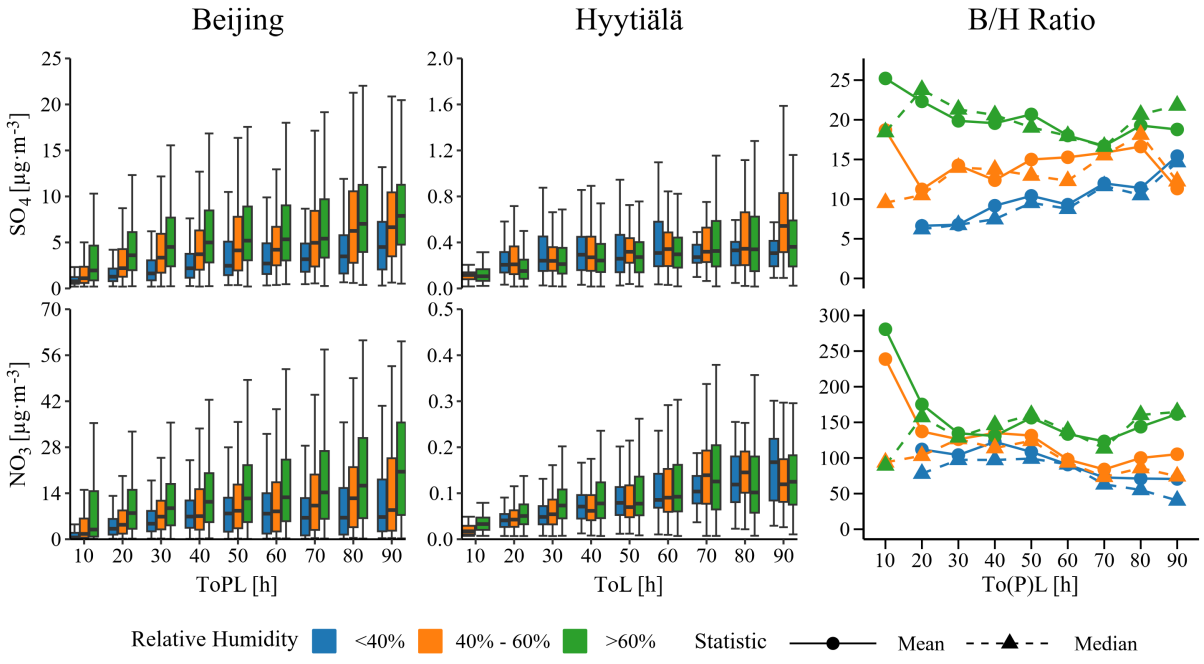


Figure 3. Sulfate and nitrate concentrations in Beijing (2018–2022) and the Hyytiälä clean-sector subset (2018–2021), grouped by RH and 10 h bins of ToPL and ToL, respectively. Bin labels indicate upper bounds. RH classes are $< 40\%$, 40–60%, and $> 60\%$. Boxes span the interquartile range, central lines indicate medians, and whiskers extend to the most extreme observations within 1.5 times the interquartile range of the corresponding quartile. Ratio panels show Beijing-to-Hyytiälä ratios of means and medians calculated separately within matching RH classes and time-bin labels. Boxes require at least 10 observations; ratios require at least 10 observations at each site.

when $\mathrm{RH} > 60\%$. The comparable NOR when $\mathrm{RH} < 40\%$ but much higher NOR ratio when $\mathrm{RH} > 60\%$ (Figure S5) further confirmed that the NO_3 formation mechanisms in Beijing and Hyytiälä were similar under low RH conditions but differed under high RH conditions.

4 Conclusions

Overall, under declining emissions, high secondary inorganic aerosol regimes in Beijing became increasingly associated with humidity and regional transport contribution, rather than precursor abundance alone. The fitted concentration–ToPL slopes under high RH were 2.7 and 1.4 times those under low RH for NO_3 and SO_4, respectively. Continued precursor reductions remain necessary. Identifying and monitoring high-risk meteorological and transport conditions that favor secondary formation and accumulation may also help improve predictions of severe SO_4 and NO_3 pollution episodes.

https://doi.org/10.5194/ar-2026-45
Preprint. Discussion started: 17 November 2026
© Author(s) 2026. CC BY 4.0 License.



AEROSOL Research Discussions

Data availability. The data supporting the findings of this study and the data sets used to reproduce the analyses and figures are available on Figshare. For peer review, the repository can be accessed through the following private link: https://figshare.com/s/9323d2c9245a2b0c6456.

Author contributions. M.K. and W.D. designed the study. Z.Z. performed the data analysis, visualization, and interpretation and wrote the original draft. W.D. and Z.Z. contributed to the interpretation of the results and substantially revised the manuscript. K.R.D. and Y.L. provided measurement resources and supervised the measurements at the Beijing site. C.Y., M.X., Q.Y., X.Z., T.Z., F.Z., Y.W., C.H., Z.W., H.P., B.S., L.M., W.Z., J.Z., L.A., I.J., N.S., T.P. and W.M. contributed to field measurements, instrument operation, data collection, and/or data quality control. G.C., J.C., Q.Z., V.-M.K., M.K., and T.K. contributed to interpretation of the results and reviewed and edited the manuscript. All authors discussed the results, commented on the manuscript, and approved the final version.

Competing interests. One of the coauthors is a member of the editorial board of Aerosol Research.

Acknowledgements. We acknowledge the following projects: ACCC Flagship funded by the Academy of Finland grant numbers 337549, 357902, 359340, 374287, Academy professorship funded by the Academy of Finland (grant no. 302958), Academy of Finland projects no. 325656, 311932, 334792, 316114, 325647, 325681, 333397, 328616, 345510, 347782, 367739, 367784 and 377242, as well as "Quantifying carbon sink, CarbonSink+ and their interaction with air quality" INAR project funded by Jane and Aatos Erkko Foundation, "Gigacity" project funded by Wihuri foundation, European Research Council (ERC) project ATM-GTP Contract No. 742206, and Horizon Europe project FOCI, grant agreement No. 101056783, and CRiceS (No 101003826), RI-URBANS (101036245), EMME-CARE (856612) and FORCeS (821205). The Technology Industries of Finland Centennial foundation via urbaani ilmanlaatu 2.0 -project is gratefully acknowledged. University of Helsinki support via ACTRIS-HY is acknowledged. Support of the technical and scientific staff in Hyytiälä and BUCT/AHL is acknowledged. Z.Z. acknowledges funding from the China Scholarship Council (grant number: 202206380019).

https://doi.org/10.5194/ar-2026-45
Preprint. Discussion started: 17 November 2026
© Author(s) 2026. CC BY 4.0 License.



References

Cao, J., Wang, Q., Chow, J. C., Watson, J. G., Tie, X., Shen, Z., Wang, P., and An, Z.: Impacts of aerosol compositions on visibility impairment in Xi'an, China, Atmos. Environ., 59, 559–566, https://doi.org/10.1016/j.atmosenv.2012.05.036, 2012.

Cao, Y., Zhang, Z., Xiao, H., Xie, Y., Liang, Y., and Xiao, H.: How aerosol pH responds to nitrate to sulfate ratio of fine-mode particulate, Environ. Sci. Pollut. Res., 27, 35 031–35 039, https://doi.org/10.1007/s11356-020-09810-0, 2020.

Ervens, B.: Modeling the processing of aerosol and trace gases in clouds and fogs, Chem. Rev., 115, 4157–4198, https://doi.org/10.1021/cr5005887, 2015.

Feng, T., Bei, N., Zhao, S., Wu, J., Liu, S., Li, X., Liu, L., Wang, R., Zhang, X., and Tie, X.: Nitrate debuts as a dominant contributor to particulate pollution in Beijing: roles of enhanced atmospheric oxidizing capacity and decreased sulfur dioxide emission, Atmos. Environ., 244, 117 995, https://doi.org/10.1016/j.atmosenv.2020.117995, 2021.

Geng, G., Xiao, Q., Zheng, Y., Tong, D., Zhang, Y., Zhang, X., Zhang, Q., He, K., and Liu, Y.: Impact of China's air pollution prevention and control action plan on $PM_{2.5}$ chemical composition over eastern China, Sci. China Earth Sci., 62, 1872–1884, https://doi.org/10.1007/s11430-018-9353-x, 2019.

Gómez-Losada, Á., Lozano-García, A., Pino-Mejías, R., and Contreras-González, J.: Finite mixture models to characterize and refine air quality monitoring networks, Sci. Total Environ., 485, 292–299, https://doi.org/10.1016/j.scitotenv.2014.03.091, 2014.

Guo, H., Liu, J., Froyd, K. D., Roberts, J. M., Veres, P. R., Hayes, P. L., Jimenez, J. L., Nenes, A., and Weber, R. J.: Fine particle pH and gas–particle phase partitioning of inorganic species in Pasadena, California, during the 2010 CalNex campaign, Atmos. Chem. Phys., 17, 5703–5719, https://doi.org/10.5194/acp-17-5703-2017, 2017.

Hakala, S., Vakkari, V., Bianchi, F., Dada, L., Deng, C., Dällenbach, K. R., Fu, Y., Jiang, J., Kangasluoma, J., Kujansuu, J., Liu, Y., Petäjä, T., Wang, L., Yan, C., Kulmala, M., and Paasonen, P.: Observed coupling between air mass history, secondary growth of nucleation mode particles and aerosol pollution levels in Beijing, Environ. Sci.: Atmos., 2, 146–164, https://doi.org/10.1039/d1ea00089f, 2022.

Han, X., Guo, Q., Lang, Y., Li, S., Li, Y., Guo, Z., Hu, J., Wei, R., Tian, L., and Wan, Y.: Seasonal and long-term trends of sulfate, nitrate, and ammonium in $PM_{2.5}$ in Beijing: implication for air pollution control, Environ. Sci. Pollut. Res., 27, 23 730–23 741, https://doi.org/10.1007/s11356-020-08697-1, 2020.

Haque, S. M., Umar, Y., and Kabir, A.: Advanced chemometric techniques for environmental pollution monitoring and assessment: a review, Chemosensors, 13, 268, https://doi.org/10.3390/chemosensors13070268, 2025.

Hari, P., Nikinmaa, E., Pohja, T., Siivola, E., Bäck, J., Vesala, T., and Kulmala, M.: Station for measuring ecosystem-atmosphere relations: SMEAR, in: Physical and Physiological Forest Ecology, edited by Hari, P., Heliövaara, K., and Kulmala, L., pp. 471–487, Springer Netherlands, Dordrecht, ISBN 978-94-007-5602-1 978-94-007-5603-8, https://doi.org/10.1007/978-94-007-5603-8_9, 2013.

Heikkinen, L., Äijälä, M., Riva, M., Luoma, K., Dällenbach, K., Aalto, J., Aalto, P., Aliaga, D., Aurela, M., Keskinen, H., Makkonen, U., Rantala, P., Kulmala, M., Petäjä, T., Worsnop, D., and Ehn, M.: Long-term sub-micrometer aerosol chemical composition in the boreal forest: inter- and intra-annual variability, Atmos. Chem. Phys., 20, 3151–3180, https://doi.org/10.5194/acp-20-3151-2020, 2020.

Kulmala, M., Wei, D., Zhang, X., Zhang, T., Xia, M., Wang, Y., Zou, Z., Zheng, F., Zhang, Y., Yang, C., Wu, J., Li, Y., Zha, Q., Yan, C., Feng, W., Wang, Z., Hua, C., Xie, J., Ma, W., Guo, Y., Chen, X., Liu, T., Li, J., Pang, H., Zhao, G., Chen, K., Zhao, Z., Zhong, W., Gao, S., Zhang, W., Yuan, Q., Qi, L., Petäjä, T., Sarnela, N., Ylivinkka, I., Aliaga, D., Cai, R., Agro, M., Ahonen, L., Schiestl-Aalto, P., Tuovinen, S., Cai, J., Kujansuu, J., Ciarelli, G., Cheng, Y., Ding, A., Dällenbach, K., Dada, L., Worsnop, D., Bianchi, F., Jiang, J., Liu, Y., Kerminen,

https://doi.org/10.5194/ar-2026-45
Preprint. Discussion started: 17 November 2026
© Author(s) 2026. CC BY 4.0 License.



V.-M., and Kokkonen, T.: Understanding atmospheric processes: insights from the comparison between Beijing and Hyytiälä, npj Clean Air, 1, 26, https://doi.org/10.1038/s44407-025-00020-x, 2025.

Land, Jr., W. H., Ford, W., Park, J.-W., Mathur, R., Hotchkiss, N., Heine, J., Eschrich, S., Qiao, X., and Yeatman, T.: Partial least squares (PLS) applied to medical bioinformatics, Procedia Comput. Sci., 6, 273–278, https://doi.org/10.1016/j.procs.2011.08.051, 2011.

Laughner, J. L. and Cohen, R. C.: Direct observation of changing NO_x lifetime in North American cities, Science, 366, 723–727, https://doi.org/10.1126/science.aax6832, 2019.

Li, Z., Sun, Y., Wang, Q., Xin, J., Sun, J., Lei, L., Li, J., Fu, P., and Wang, Z.: Nitrate and secondary organic aerosol dominated particle light extinction in Beijing due to clean air action, Atmos. Environ., 269, 118 833, https://doi.org/10.1016/j.atmosenv.2021.118833, 2022.

Liu, P., Ye, C., Xue, C., Zhang, C., Mu, Y., and Sun, X.: Formation mechanisms of atmospheric nitrate and sulfate during the winter haze pollution periods in Beijing: gas-phase, heterogeneous and aqueous-phase chemistry, Atmos. Chem. Phys., 20, 4153–4165, https://doi.org/10.5194/acp-20-4153-2020, 2020a.

Liu, T., Chan, A. W. H., and Abbatt, J. P. D.: Multiphase oxidation of sulfur dioxide in aerosol particles: implications for sulfate formation in polluted environments, Environ. Sci. Technol., 55, 4227–4242, https://doi.org/10.1021/acs.est.0c06496, 2021a.

Liu, Y., Wu, Z., Wang, Y., Xiao, Y., Gu, F., Zheng, J., Tan, T., Shang, D., Wu, Y., and Zeng, L.: Submicrometer particles are in the liquid state during heavy haze episodes in the urban atmosphere of Beijing, China, Environ. Sci. Technol. Lett., 4, 427–432, https://doi.org/10.1021/acs.estlett.7b00352, 2017.

Liu, Y., Yan, C., Feng, Z., Zheng, F., Fan, X., Zhang, Y., Li, C., Zhou, Y., Lin, Z., Guo, Y., Zhang, Y., Ma, L., Zhou, W., Liu, Z., Dada, L., Dällenbach, K., Kontkanen, J., Cai, R., Chan, T., Chu, B., Du, W., Yao, L., Wang, Y., Cai, J., Kangasluoma, J., Kokkonen, T., Kujansuu, J., Rusanen, A., Deng, C., Fu, Y., Yin, R., Li, X., Lu, Y., Liu, Y., Lian, C., Yang, D., Wang, W., Ge, M., Wang, Y., Worsnop, D. R., Junninen, H., He, H., Kerminen, V.-M., Zheng, J., Wang, L., Jiang, J., Petäjä, T., Bianchi, F., and Kulmala, M.: Continuous and comprehensive atmospheric observations in Beijing: a station to understand the complex urban atmospheric environment, Big Earth Data, 4, 295–321, https://doi.org/10.1080/20964471.2020.1798707, 2020b.

Liu, Y., Feng, Z., Zheng, F., Bao, X., Liu, P., Ge, Y., Zhao, Y., Jiang, T., Liao, Y., and Zhang, Y.: Ammonium nitrate promotes sulfate formation through uptake kinetic regime, Atmos. Chem. Phys., 21, 13 269–13 286, https://doi.org/10.5194/acp-21-13269-2021, 2021b.

Mahieu, B., Qannari, E. M., and Jaillais, B.: Extension and significance testing of variable importance in projection (VIP) indices in partial least squares regression and principal components analysis, Chemom. Intell. Lab. Syst., 242, 104 986, https://doi.org/10.1016/j.chemolab.2023.104986, 2023.

Meng, F., Zhang, Y., Kang, J., Heal, M. R., Reis, S., Wang, M., Liu, L., Wang, K., Yu, S., and Li, P.: Trends in secondary inorganic aerosol pollution in China and its responses to emission controls of precursors in wintertime, Atmos. Chem. Phys., 22, 6291–6308, https://doi.org/10.5194/acp-22-6291-2022, 2022.

National Centers for Environmental Prediction: Global Data Assimilation System (GDAS1) one-degree meteorological archive, https://www.ready.noaa.gov/gdas1.php, n.d.

Neefjes, I., Laapas, M., Liu, Y., Médus, E., Miettunen, E., Ahonen, L., Quéléver, L., Aalto, J., Bäck, J., Kerminen, V.-M., Lampilahti, J., Luoma, K., Mäki, M., Mammarella, I., Petäjä, T., Räty, M., Sarnela, N., Ylivinkka, I., Hakala, S., Kulmala, M., Nieminen, T., and Lintunen, A.: 25 years of atmospheric and ecosystem measurements in a boreal forest - seasonal variation and responses to warm and dry years, Boreal Environ. Res., 27, 1–31, http://urn.fi/URN:NBN:fi-fe2022102062634, 2022.

https://doi.org/10.5194/ar-2026-45
Preprint. Discussion started: 17 November 2026
© Author(s) 2026. CC BY 4.0 License.

Petäjä, T., Tabakova, K., Manninen, A., Ezhova, E., O'Connor, E., Moisseev, D., Sinclair, V. A., Backman, J., Levula, J., and Luoma, K.: Influence of biogenic emissions from boreal forests on aerosol–cloud interactions, Nat. Geosci., 15, 42–47, https://doi.org/10.1038/s41561-021-00876-0, 2022.

Righi, C., Ciobanu, M., Deot, N., Jokinen, T., Liu, C., Yuan, Q., Quéléver, L. L. J., Jorga, S., Pospisilova, V., Beck, L. J., Simon, M., Zauner-Wieczorek, M., Kürten, A., Soler, R., Vera, T., Muñoz, A., Ahonen, L. R., Yan, C., Petäjä, T., and Sarnela, N.: Towards harmonized measurements of condensable vapors: insights from the intercomparison of six chemical ionization mass spectrometers at a boreal forest site, Atmos. Meas. Tech., 19, 6357–6378, https://doi.org/10.5194/amt-19-6357-2026, 2026.

Stein, A. F., Draxler, R. R., Rolph, G. D., Stunder, B. J. B., Cohen, M. D., and Ngan, F.: NOAA's HYSPLIT atmospheric transport and dispersion modeling system, Bull. Am. Meteorol. Soc., 96, 2059–2077, https://doi.org/10.1175/BAMS-D-14-00110.1, 2015.

Sun, Y., Lei, L., Zhou, W., Chen, C., He, Y., Sun, J., Li, Z., Xu, W., Wang, Q., and Ji, D.: A chemical cocktail during the COVID-19 outbreak in Beijing, China: insights from six-year aerosol particle composition measurements during the Chinese New Year holiday, Sci. Total Environ., 742, 140 739, https://doi.org/10.1016/j.scitotenv.2020.140739, 2020.

Tunved, P., Hansson, H.-C., Kerminen, V.-M., Ström, J., Maso, M. D., Lihavainen, H., Viisanen, Y., Aalto, P. P., Komppula, M., and Kulmala, M.: High natural aerosol loading over boreal forests, Science, 312, 261–263, https://doi.org/10.1126/science.1123052, 2006.

Vasilakos, P., Russell, A., Weber, R., and Nenes, A.: Understanding nitrate formation in a world with less sulfate, Atmos. Chem. Phys., 18, 12 765–12 775, https://doi.org/10.5194/acp-18-12765-2018, 2018.

Wang, J., Gao, J., Che, F., Wang, Y., Lin, P., and Zhang, Y.: Decade-long trends in chemical component properties of $PM_{2.5}$ in Beijing, China (2011–2020), Sci. Total Environ., 832, 154 664, https://doi.org/10.1016/j.scitotenv.2022.154664, 2022a.

Wang, J., Gao, J., Che, F., Wang, Y., Lin, P., and Zhang, Y.: Dramatic changes in aerosol composition during the 2016–2020 heating seasons in Beijing–Tianjin–Hebei region and its surrounding areas: the role of primary pollutants and secondary aerosol formation, Sci. Total Environ., 849, 157 621, https://doi.org/10.1016/j.scitotenv.2022.157621, 2022b.

Wang, J., Han, Y., Yu, X., Zhang, Z., and Song, T.: Improvements on Gaussian mixture model and its application in identifying aerosol types in two major cities in the Yangtze River Delta, China, Sci. Total Environ., 935, 172 743, https://doi.org/10.1016/j.scitotenv.2024.172743, 2024.

Wang, T., Liu, Y., Zhou, S., Wang, G., Liu, X., Wang, L., Fu, H., Chen, J., and Zhang, L.: Key factors determining the formation of sulfate aerosols through multiphase chemistry—a kinetic modeling study based on Beijing conditions, J. Geophys. Res.: Atmos., 128, e2022JD038 382, https://doi.org/10.1029/2022jd038382, 2023.

Wang, Y., Gao, W., Wang, S., Song, T., Gong, Z., Ji, D., Wang, L., Liu, Z., Tang, G., and Huo, Y.: Contrasting trends of $PM_{2.5}$ and surface-ozone concentrations in China from 2013 to 2017, Natl. Sci. Rev., 7, 1331–1339, https://doi.org/10.1093/nsr/nwaa032, 2020.

Xie, F., Su, Y., Tian, Y., Shi, Y., Zhou, X., Wang, P., Yu, R., Wang, W., He, J., and Xin, J.: The shifting of secondary inorganic aerosol formation mechanisms during haze aggravation: the decisive role of aerosol liquid water, Atmos. Chem. Phys., 23, 2365–2378, https://doi.org/10.5194/acp-23-2365-2023, 2023.

Xie, Y., Zha, Q., Liu, T., Liu, H., Yin, J., Liu, Y., Wang, J., Qi, X., Zhu, C., Nie, W., Chi, X., Huang, X., and Ding, A.: Alpine wetlands as an overlooked source of dimethyl sulfide (DMS) on the Tibetan Plateau, Environ. Sci. Technol. Lett., 13, 803–810, https://doi.org/10.1021/acs.estlett.6c00135, 2026.

Xu, W., Liu, X., Liu, L., Dore, A. J., Tang, A., Lu, L., Wu, Q., Zhang, Y., Hao, T., and Pan, Y.: Impact of emission controls on air quality in Beijing during APEC 2014: implications from water-soluble ions and carbonaceous aerosol in $PM_{2.5}$ and their precursors, Atmos. Environ., 210, 241–252, https://doi.org/10.1016/j.atmosenv.2019.04.050, 2019.

https://doi.org/10.5194/ar-2026-45
Preprint. Discussion started: 17 November 2026
© Author(s) 2026. CC BY 4.0 License.



Yu, Y., Dai, C., Wei, Y., Ren, H., and Zhou, J.: Air pollution prevention and control action plan substantially reduced $PM_{2.5}$ concentration in China, Energy Econ., 113, 106 206, https://doi.org/10.1016/j.eneco.2022.106206, 2022.

Zhang, R., Wang, G., Guo, S., Zamora, M. L., Ying, Q., Lin, Y., Wang, W., Hu, M., and Wang, Y.: Formation of urban fine particulate matter, Chem. Rev., 115, 3803–3855, https://doi.org/10.1021/acs.chemrev.5b00067, 2015.

Zheng, B., Tong, D., Li, M., Liu, F., Hong, C., Geng, G., Li, H., Li, X., Peng, L., and Qi, J.: Trends in China's anthropogenic emissions since 2010 as the consequence of clean air actions, Atmos. Chem. Phys., 18, 14 095–14 111, https://doi.org/10.5194/acp-18-14095-2018, 2018.